Polarons and soliton pairs (bipolarons) in halogen-doped quasi-one-dimensional mixed-valence platinum complexes

M. Haruki and S. Kurita
Laboratory of Applied Physics, Faculty of Engineering,
Yokohama National University, Hodogaya, Yokohama 240, Japan
(Received 13 September 1988)

The first experimental studies on halogen doping in quasi-one-dimensional, halogen-bridged, mixed-valence platinum complexes (HMPC) are presented. The electrical conductivity of the iodine compound increases over 7 orders of magnitude with iodine doping. The absorbance of the two optical-absorption bands near the midgap and the ESR intensity in dilute doped HMPC increase with the dopant concentration. In the dilute regime, halogen doping yields the same effects on optical absorption and ESR as does photoexcitation at an energy greater than or equal to the energy of the charge-transfer absorption band. The doping-induced states are located on single chains and have charge and spin. These results strongly suggest polaron formation by halogen doping. At high doping levels, a new doping-induced absorption appears at an energy of 1.55 eV at 77 K, and the ESR decreases in intensity as the doping proceeds. It appears that upon halogen doping, singly charged polarons are produced and the formation of confined charged soliton pairs (bipolarons) via the process $P^+ + P^+ \rightarrow S^+ + S^+$ (or B^{2+}) is favored.

I. INTRODUCTION

Recently, there has been a growing interest in nonlinear excitations in quasi-one-dimensional, mixed-valence materials,[1-9] which comprise linear chains $(\cdots M^{2+}\text{—}X\text{—}M^{4+}\text{—}X\cdots)_n$ composed of transition metal (M=Pt,Pd,Ni) complexes bridged by a halogen atom (X=Cl,Br,I). Halogen-bridged, mixed-valence metal complexes are highly anisotropic crystalline solids, exhibiting strongly dicroic absorption in the visible region attributed to the $M^{2+}\rightarrow M^{4+}$ intervalence charge-transfer (CT) transitions.[10] The ground-state configuration has a twofold degeneracy which allows for solitonlike excitations,[1,2] and is characterized as a charge-density wave (CDW) arising from a charge disproportionation on the sites of the M sublattice accompanying substantial distortion of the X sublattice. This is in contrast to the case of a conjugated polymer in which a bond-order-wave (BOW) ground state appears.[11] Consequently, we expect the appearance of interesting nonlinear excitation phenomena in halogen-bridged complexes resulting from the strong electron-phonon interaction. Baeriswyl and Bishop[3] have calculated intrinsic defect states (solitons, polarons, bipolarons, and excitons) in the strong CDW limit and demonstrated that they are strongly localized in the MX chain, in contrast to the relatively extended defect states in a conjugated polymer. The soliton mass in the MX chain has been estimated to be several hundred times as much as that of solitons in *trans*-polyacetylene.[2] This suggests that solitons (and the other excitation species) in the MX chain are far less mobile than in *trans*-polyacetylene.

Nonlinear excitation states can be generated by photoexcitation.[12] For halogen-bridged, mixed-valence metal complexes it is expected that soliton-antisoliton or polaron pairs can be produced in the relaxation process of the CT excited states $\cdots X\text{—}M^{3+}\text{—}X\text{—}M^{3+}\text{—}X\cdots$ on the MX chain. If such photogenerated carrier pairs are widely separated, they will have a long lifetime because their masses are too heavy to move for recombination. In fact, long-lived photoinduced absorption[6-8] and photoinduced electron-spin resonance (ESR)[8] in halogen-bridged, mixed-valence platinum complexes have been observed when photoexcitation has been made in the region of the CT absorption band or above. The absorption and ESR are induced only for the excitation with light polarized parallel to the chain, and the photoinduced absorption is polarized parallel to the chain axis, suggesting that the photogenerated carriers are located on single chains. The photoinduced absorption bands (A and B bands in Ref. 7) are observed near the midgap, and the photogenerated carriers have both spin and charge. From these experimental results, polarons have been proposed as photogenerated carriers.[7] Very recently, Nasu and Mishima[9] have shown that a part of the carriers generated by light of higher photon energy than the band gap results in forming stable, widely separated polaron pairs; this is an origin of photoinduced absorption. Such a photoinduced defect state (polaron), located on the MX chain, is depicted as $\cdots M^{2+}\text{—}X\text{—}M^{4+}\text{—}X\text{—}M^{3+}\text{—}X\text{—}M^{4+}\cdots$. This configuration may be produced by halogen doping. In halogen-bridged, mixed-valence metal complexes, an added hole (electron) will create an M^{3+} state on the MX chain,

P^+: $\cdots\text{—}M^{2+}\text{—}X\text{—}M^{4+}\text{—}X\text{—}M^{3+}\text{—}X\text{—}M^{4+}\text{—}X\text{—}M^{2+}\text{—}\cdots$

(P^-: $\cdots\text{—}M^{2+}\text{—}X\text{—}M^{3+}\text{—}X\text{—}M^{2+}\text{—}X\text{—}M^{4+}\text{—}X\text{—}M^{2+}\text{—}\cdots$).

and give rise to lattice deformation around the defect states. Such defect states, produced by doping with acceptors or donors, can be regarded as positively charged (P^+) or negatively charged (P^-) polarons, respectively. This means that information on nonlinear excitations may be obtained from doping experiments as well as from photoexcitation.

We have successfully carrier out halogen doping in $(Pt(en)_2)(Pt(en)_2X_2)(ClO_4)_4$ (en=ethylenediamine, X=Cl or I; we refer to this complex as Pt-X) which is one of typical halogen-bridged, mixed-valence metal complexes. To our knowledge this is the first intentional halogen-doping in compounds of this class.

We report, in this paper, the effects of halogen doping on the electrical, optical, and magnetic properties of Pt-X. We find that the electrical conductivity of halogen doped Pt-I increases by 7 orders of magnitude and that doping-induced absorption and ESR are also observed in Pt-X. At high doping levels, the ESR intensity decreases and a new absorption band appears near the midgap. These results are discussed within the framework of polaron and charged soliton or bipolaron models.

II. EXPERIMENTAL DETAILS AND RESULTS

A. Halogen doping

The single crystals of $(Pt(en)_2)(Pt(en)_2X_2)(ClO_4)_4$ (X=Cl,I) used in this study were prepared using the techniques reported by Baslo *et al.*[13] and by Bekaloglu *et al.*[14]

Halogen doping was carried out by exposing the single crystals in a glass vessel to halogen vapor. For chlorine doping 1 atm of chlorine gas was directly injected into the glass vessel (150 ml) at room temperature and the contents allowed to react. For iodine doping, 50 mg of iodine was introduced into the vessel by the trap-to-trap method; subsequently, the vessel was heated to 50 °C. The contents of dopant chlorine in Pt-Cl were determined for some of the samples by chemical analysis. The results were as follows: for Pt-Cl:Cl_y, y=6 mol % for a 9-h reaction, and y=9 mol % for a 14-h reaction.[15] The contents of dopant iodine and chlorine in Pt-I were not determined. Hence, in this study all levels of doping were evaluated by the reaction time and the reaction temperature. The colors of Pt-Cl and Pt-I crystals doped with chlorine at room temperature for 7 days changed from red to nondichroic orange and from lustrous gold to nondichroic black, respectively. The nondichroic colors of such heavily doped crystals hardly changed after removal of the halogen vapor by vacuum pumping for 24 h. This is in contrast to the lightly doped crystals which recover in vacuum, showing that the heavily doped crystals are damaged on exposure to halogen gas for such a long time. In our study, since the doping times were less than 48 h, the samples maintained their crystalline properties.

B. Electrical dc conductivity

Measurements of dc conductivity were carried out using four-probe techniques. Gold wires and Electrodag were used to make electrical contacts to the samples, and the contacts were checked to be Ohmic. The typical applied electric field was about 500 $V\,cm^{-1}$. Room-temperature conductivity of Pt-I was typical of earlier results,[16] $\sigma \sim 10^{-8}\ \Omega^{-1}\,cm^{-1}$. All measurements were performed by using a high-impedance electrometer (Keithley 610C with an input impedance $>10^{14}\Omega$). Because the dopant could be removed easily from the crystals through pumping (especially for light doping levels), the electrical contacts were applied before doping and conductivity measurements were made in the atmosphere of a halogen gas. Electrical conductivities were measured primarily on Pt-I because the resistivity of the Pt-Cl samples was too high for our instruments.

Figure 1 shows the electrical conductivity of Pt-I during the doping reaction with iodine at 50 °C. In the figure the open and solid circles denote the conductivities parallel and perpendicular to the chain axis, respectively. The conductivities parallel- ($\sigma_\parallel$) and perpendicular- ($\sigma_\perp$) to-chain increased by approximately 4 and 7 orders of magnitude, respectively, during iodine doping. After a doping reaction for 15 h, each conductivity approached the maximum value of $\sigma_\parallel \sim 4\times10^{-3}$ and $\sigma_\perp \sim 5\times10^{-2}$ $\Omega^{-1}\,cm^{-1}$. It should be noted that $\sigma_\parallel$ is smaller than $\sigma_\perp$ after doping, though $\sigma_\parallel$ is larger than $\sigma_\perp$ before doping. The increase in conductivity by 4 orders of magnitude was also observed in chlorine-doped Pt-I (Fig. 2). The conductivity of Pt-I doped for 12 h was reduced to that of undoped crystals after pumping for 2 h. When the conductivity measurements were carried out in Pt-Cl, the sample was heated up to 80 °C because of the quite low

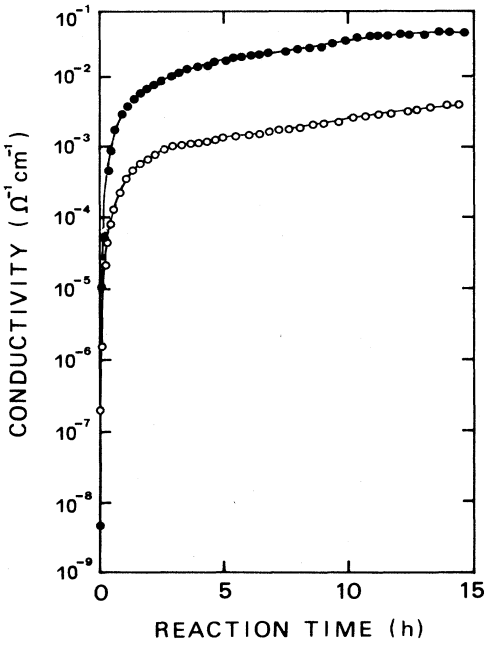

FIG. 1. Electrical conductivities of $(Pt(en)_2)(Pt(en)_2I_2)(ClO_4)_4$ during doping reaction with iodine at 50 °C. Parallel- and perpendicular-to-chain conductivities are represented by open and solid circles, respectively.

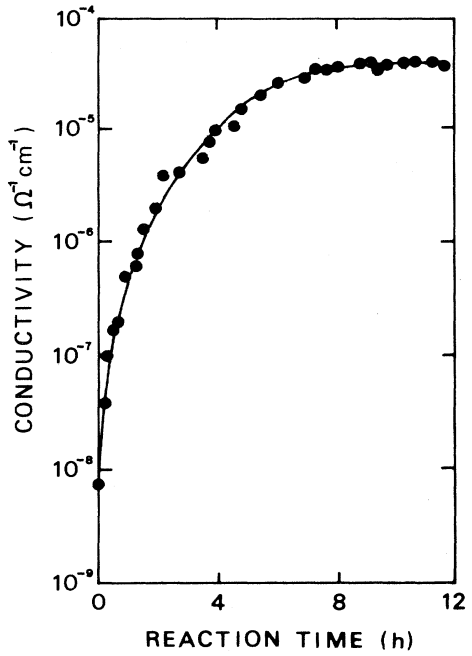

FIG. 2. Parallel-to-chain conductivity of $(Pt(en)_2)(Pt(en)_2I_2)(ClO_4)_4$ during doping reaction with chlorine at room temperature.

conductivity at room temperature. The conductivity at 80 °C of chlorine-doped Pt-Cl increased about 1 order of magnitude after 15 h of the doping reaction, and its value was unchanged after 2 days of doping reaction.

C. Optical absorption

The optical-absorption measurements were carried out by the transmission method on chlorine-doped Pt-Cl (thickness ~ 40 μm) at room temperature. The samples were mounted in a glass vessel which contained 1 atm of chlorine gas in order to measure the optical absorption without changing the experimental configuration and without exposing the sample to air.

Figure 3 shows the optical-absorption spectra of chlorine-doped Pt-Cl for polarization parallel to the chain axis: curve 1, undoped; curves 2, 3, and 4 are for doping reaction times (t) of 0.5, 1.5, and 16 h, respectively. P is the absorption edge of the CT absorption band. All absorption spectra in the figure were measured on the same sample. At light doping levels ($t \leq 0.5$ h) the A (and B) bands grew with the time of reaction. For $t \geq 0.5$ h, the peak position of the A band shifted slightly toward lower energy and the absorption intensity near 1.85 eV decreased. Curve 5 indicates the difference in optical-absorption intensities between curves 1 and 4. The maximum in curve 5 near 1.5 eV suggests that a new absorption peak appears at high doping levels. In order to separate this new band from the A and B bands more precisely, the absorption spectra of doped Pt-Cl were measured at 77 K. Figure 4 shows the optical-absorption spectrum of Pt-Cl at 77 K, before (dotted line) and after the doping with chlorine for 4 h at 20 °C (solid line). The

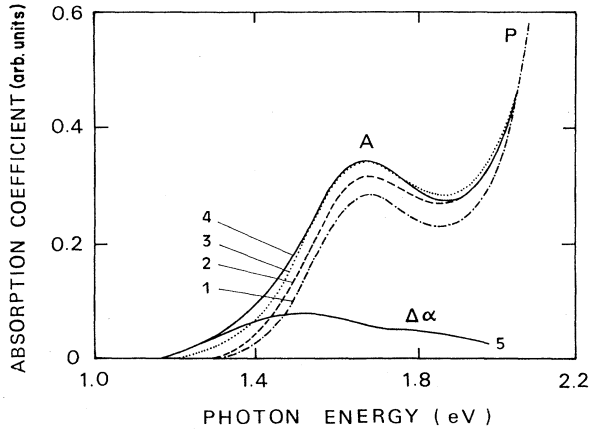

FIG. 3. Chlorine-doping-induced absorption spectra of $(Pt(en)_2)(Pt(en)_2Cl_2)(ClO_4)_4$ for the polarization parallel to the chain axis at room temperature: undoped (curve 1); reaction time of 0.5 h (curve 2); 1.5 h (curve 3); 16 h (curve 4); the difference in absorption intensities between curve 1 and 4 is shown (curve 5).

peak position of the A band was changed from 1.68 to 1.60 eV by doping; however, that of the B band was unchanged. As A and B bands originate from the same defects,[7] a new band spectrum can be derived by subtracting the undoped Pt-Cl absorption intensity from the doped one. The dashed line indicates the difference in the optical-absorption intensities between doped and undoped Pt-Cl. The result indicates that at 77 K, new doping-induced absorption appears at 1.55 eV for high doping levels. There was no doping-induced absorption for polarization perpendicular to the chain.

D. Electron-spin resonance

ESR measurements were carried out by using a JEOL JES-FE1XG ESR spectrometer at X-band with a modula-

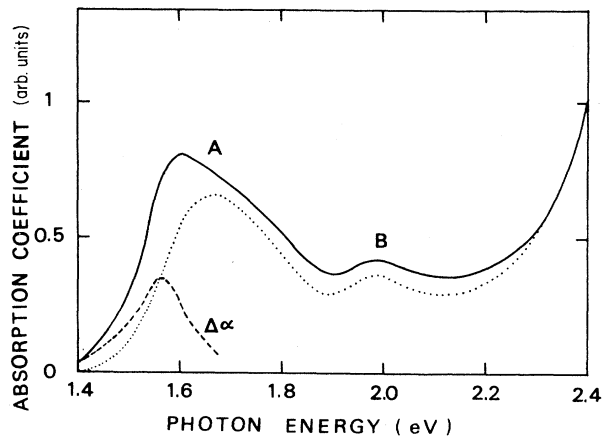

FIG. 4. Chlorine-doping-induced absorption spectra of $(Pt(en)_2)(Pt(en)_2Cl_2)(ClO_4)_4$ for the polarization parallel to the chain axis at 77 K: undoped (dotted line); doping reaction for 4 h (solid line). The dashed line denotes the difference in absorption intensities between undoped and 4-h-doped crystals.

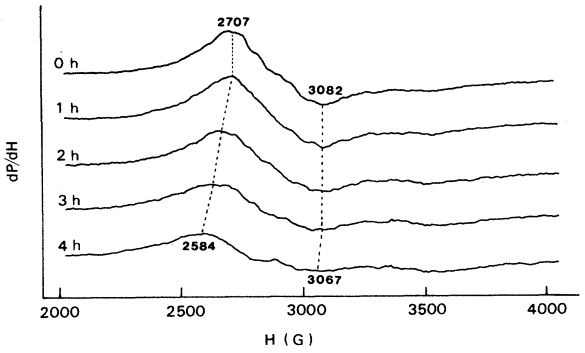

FIG. 5. The derivative curve of ESR in chlorine-doped $(Pt(en)_2)(Pt(en)_2Cl_2)(ClO_4)_4$ at room temperature as a function of doping reaction time for a modulation amplitude of 2 G and microwave power 30 mW with the magnetic field perpendicular to the chain axis.

tion field of 2 G at 100 kHz. The resonance magnetic field was calibrated using a proton-NMR Gaussmeter. All samples were loaded into the quartz ESR tube in such a way that the chain axes were directed perpendicular to the resonance magnetic field. The weights of the specimens were about 150 mg. ESR signals were monitored at room temperature during the doping process.

The derivative curves of ESR in chlorine-doped Pt-Cl are shown in Fig. 5, where the ESR was measured at room temperature as a function of the doping time. The peaks shifted with doping and the linewidth broadened by almost 100 G after a 4-h doping reaction. These changes in ESR spectra were restored by pumping. The ESR intensities of (a) Pt-Cl and (b) Pt-I were plotted as a function of reaction time (Fig. 6). At first, ESR intensities increased slightly ($t \leq 1$ h) and then decreased. It should be noted that, in contrast to photoinduced ESR signals, which saturate under strong photoexcitation,[8]

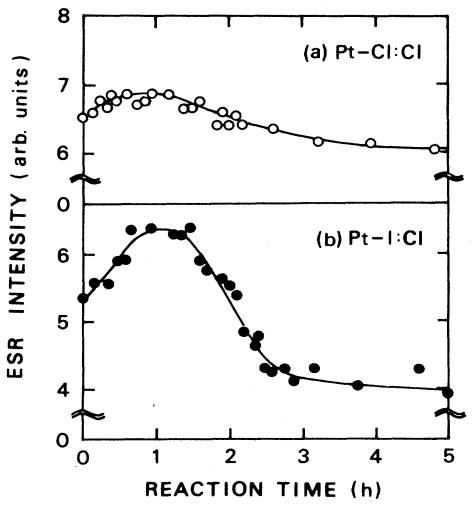

FIG. 6. Doping-induced ESR intensities of $(Pt(en)_2)(Pt(en)_2X_2)(ClO_4)_4$ (X=Cl,I) as a function of doping reaction time.

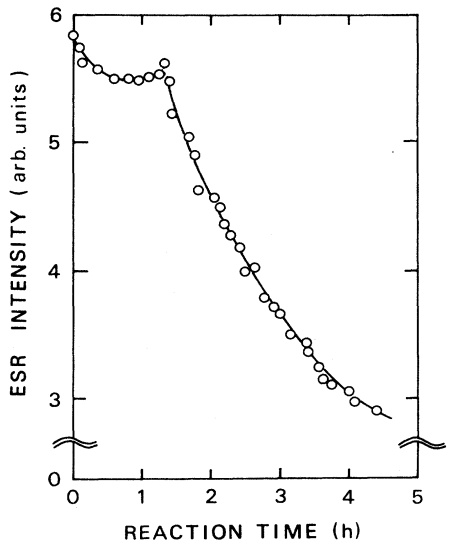

FIG. 7. Doping-induced ESR intensity of $(Pt(en)_2)(Pt(en)_2Cl_2)(ClO_4)_4$ photoexcited before doping. The photoexcitation was made by using a Hg lamp with a glass filter through the window of cavity for 1 h at 77 K.

doping-induced ESR signals were reduced at high doping levels.

In order to obtain information concerning doping- and photoinduced defects, we measured the doping-induced ESR at room temperature on a sample which was irradiated for 1 h at 77 K by a 500 W Hg lamp with a filter which cut out the visible part of the spectrum. The result is shown in Fig. 7. In the case of the photoexcited sample, a slight decrease in ESR intensity was observed at first. After that, the ESR signal remained constant until 1.2 h, and then decreased again.

III. DISCUSSION

The increases in the electrical conductivities (Figs. 1 and 2) and ESR intensities (Fig. 6) at dilute doping levels indicate the formation of charged carriers with spin. These results demonstrate that the doping-induced carriers are not charged solitons.

The remarkable increase in perpendicular-to-chain conductivity of doped Pt-I shows that the doping-induced carriers can move between chains as well as along chains. The carriers may hop between chains by utilizing the dopant ions (X^-) as intermediate sites; that is, the dopants produce new paths connecting the chains. This may explain the experimental result that the perpendicular-to-chain conductivity of doped Pt-I becomes comparable to the parallel one, in contrast to the results for undoped Pt-I. Since the conductivity is proportional to the number of paths ($\propto$ mobility) as well as to the number of carriers, the perpendicular-to-chain conductivity increases more rapidly with the dopant concentration than the parallel one. The large increase in perpendicular-to-chain conductivity that is observed may be experimental evidence that the dopants are located between chains.

Photoinduced absorption and ESR experiments have shown that the photoinduced defect states are polaron pairs, in the form of M^{3+} states on M^{2+}—M^{4+} chains: X—M^{4+}—X—M^{3+}—X—M^{4+}—X for a positive polaron P^+ and X—M^{2+}—X—M^{3+}—X—M^{2+}—X for a negative polaron P^-.[7] The polaron pair (P^+-P^-) on the chain is quite stable at low temperatures because of its heavy mass. At high temperatures, the polaron becomes mobile, leading to the recombination of polaron pairs. This explains why the photoinduced absorption and ESR are observed only at low temperatures.

The doped halogen may remove one of the electrons from the outer shell of the Pt^{2+} ion, resulting in the formation of Pt^{3+} states. If Pt^{3+} states are formed on the Pt-X chain, lattice deformation and charge distribution arise around the Pt^{3+} states. Such defect states can be regarded as positively charged polarons pinned to the dopant ions.

The experimental results show that with halogen doping and photoexcitation,[7,8] the induced optical absorption observed near midgap and the induced ESR signal have quite similar spectral shapes, energy positions, and g factors. Thus, we conclude that the halogen-doping-induced and photogenerated carriers are the same species, that is, polarons. Since the chains in Pt-X complexes are separated from each other by ~ 9 Å and ligand molecules are located between the dopant and the Pt-X chain, the interaction between the dopant and the polarons will be weak and the polarons may not be affected by the dopant. This is the reason why doping and photoexcitation yield the same features in ESR and absorption spectra.

The photoinduced absorption bands have shown temperature quenching.[7] The photoinduced absorption spectrum of the sample which was kept at room temperature for 4 h after the photoexcitation at 77 K, however, did not return to the spectrum before the photoexcitation (Figs. 3 and 4 in Ref. 7). This result suggests that a small number of polaron pairs (P^+-P^-) remain near the surface of the sample at room temperature. If halogen doping is carried out in such a sample, the halogen dopant will initially remove an electron from P^-. As a result, the P^- state (Pt^{2+}—X—Pt^{3+}—X—Pt^{2+}) may be reduced to the ground state (Pt^{2+}—X—Pt^{4+}—X—Pt^{2+}), thus decreasing the number of polarons that could contribute to the ESR absorption. As seen in Fig. 7, the doping-induced ESR intensity of Pt-Cl, which was irradiated at 77 K before doping, decreased during the initial reaction. This result is in agreement with our expectation and supports the polaron model of photoexcitation and doping. The plateau in Fig. 7 that occurs after a long reaction is explained by the balance between the reduction of the P^- state and the production of the P^+ state by halogen doping.

The A and B absorption bands ascribed to doping-induced and photogenerated carriers have been observed in undoped crystals, suggesting that a small number of polarons already exist in as-grown crystals. We expect that excess (or less) halogen atoms are introduced in the process of synthesis because exactly equimolar solutions of the Pt^{4+} complex and the Pt^{2+} complex may not have been mixed.

The density of photogenerated polaron pairs increases with the photoexcitation intensity. The high density of polaron pairs, however, leads to a higher probability of recombination of P^+ and P^-. In fact, the intensities of photoinduced absorption and ESR appear to saturate for strong photoexcitation. On the other hand, singly charged carriers (positive polarons) are formed by halogen doping. At high doping levels there will be some possibility that other kinds of carriers are produced by the reactions among the polarons, for example,

$$P^+ + P^+ \rightarrow S^+ + S^+$$

or

$$P^+ + P^+ \rightarrow B^{2+} ,$$

where S^+ denotes a soliton and B^{2+} denotes a bipolaron charged positively. Thus, the fundamental differences between doping and photoexcitation can be seen at high doping levels. Unfortunately, in this study the dopant concentrations are not determined quantitatively. Nevertheless, they can be estimated qualitatively in terms of the doping reaction times. In this study, the spectral features in ESR and optical absorption of the chlorine-doped crystals have changed after a doping reaction of one hour. Hence, in this discussion we can assume that the dopant concentration obtained in about one hour of reaction corresponds to a critical one, below which singly charged carriers on individual chains may be present without mutual interaction. As the amount of the injected dopant increases, the polaron density reaches a critical point, at which it is more favorable for the positive polarons to pair up as positive solitons or bipolarons. The available experimental evidence of soliton or bipolaron formation at high doping levels is the following: (1) a new absorption band has been observed at an energy of 1.55 eV, (2) the ESR intensity has fallen (new carriers have no spin), and (3) conductivity has increased (new carriers are mobile and have charge). As discussed later, solitons or bipolarons show an absorption band near the midgap. It is very likely that the new absorption band observed at 1.55 eV can be ascribed to this midgap absorption.

Figure 8 shows a schematic diagram of a positively charged kink (soliton) on the MX chain and a corresponding energy-level diagram[3] for the strong electron-phonon coupling regime. According to the model proposed by Baeriswyl and Bishop,[3,4] an optical transition occurs at $1.5\Delta - U + V$ for a kink soliton (Fig. 8) and a bi-

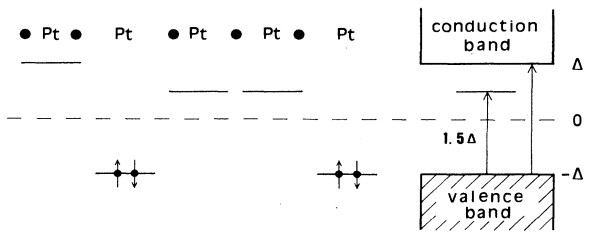

FIG. 8. Energy-level diagram and associated Pt-X displacement pattern for a positively charged kink (soliton). The solid circles denote halogen ions.

TABLE I. Summary of principal results on halogen doping and photoexcitation (Refs. 7 and 8) in $(Pt(en)_2)(Pt(en)_2X_2)(ClO_4)_4$, ($X$=Cl,I). (RT denotes room temperature.)

	Halogen doping		Photoexcitation[a]	
	Light	Heavy	RT	77 K
Spin density	increase	decrease	unchanged	increased
Conductivity	increase	increase	slight increase ($\sim$250 K)	
Midgap state (α)				
1.68 (2.0) eV	increase		unchanged	increase
1.55 eV		appearance		

[a]References 7 and 8.

polaron, and the creation energy of two solitons is the same as that of a bipolaron. The CT exciton absorption band is located at $2\Delta - U + 3V$. Here $\Delta = 2\beta^2/K$ is the order parameter with electron-phonon coupling constant β and a harmonic spring constant K, the U and V are the Coulomb energies between the electrons on the same site and between the nearest-neighbor sites, respectively.

For Pt-Cl the experimentally determined parameters are $V = \beta/K = 0.384$ Å for the lattice distortion and $\omega_0 = (2K/M)^{1/2} = 310$ cm^{-1} for the Raman-active stretching mode, where M is the chlorine mass. Using these parameters, we obtain 1.9 eV for Δ. If the new absorption band induced by doping is due to a kink soliton (Fig. 8), we find $U = 1.4$ eV and $V = 0.1$ eV for the observed value of the CT exciton band of 2.7 eV.[17] However, these parameters cannot reproduce the absorption bands originating from polarons, predicted by Baeriswyl and Bishop, which are given as $1.75\Delta - U + 2V$ and $1.25\Delta + 2V$.

We can check more directly whether the Baeriswyl and Bishop model in the strong-coupling limit is applicable for Pt-Cl. One method is to measure the band gap. The band-gap energy, given by 2Δ in this model, is determined experimentally in terms of the threshold energy of photoconduction. We have measured the photoconduction of Pt-Cl at room temperature and found that the onset occurs near 3.1 eV. This observed optical gap is smaller than the calculated gap of 3.8 eV. This discrepancy may imply that Pt-Cl does not belong to the strong-coupling regime; that is, the transfer energy may be appreciable in halogen-bridged, mixed-valence platinum complexes.[17,18]

Recently, Nasu and Mishima[9] calculated the ground and excited states with the one-dimensional extended Peierls-Hubbard model. They have shown that the CT state created by a higher photon energy than the band gap relaxes to the excited states of the self-trapped exciton and then is partially dissociated into a separated polaron pair, i.e., a positive polaron and a negative polaron. These polarons will show three absorption bands, two of which may be seen at the energies of 70% and 80% of the band gap. Thus, Nasu and Mishima have assigned the A and B bands as the excitation of these polaron states. In addition, they have shown that the extent of the polaron is about 6 times the lattice constant. This calculated value suggests that Pt-X is in the intermediate-coupling regime.

In conclusion, we have presented the first experimental study of the polaron and confined soliton-pair (bipolaron) formation upon halogen doping in quasi-one-dimensional, mixed-valence platinum complexes with a degenerate ground state. Theoretical analysis[3] has demonstrated that a charged soliton represents the lowest-energy configuration for an excess charge on an MX chain; however, we have supposed that the charged polaron is initially formed by the removal of an electron from Pt^{2+} by halogen doping. In the dilute doping regime the results of the conductivity experiments have shown that charged carriers are generated by doping. Furthermore, ESR experiments have shown that these carriers have spin.

Two additional absorption features have appeared below the gap, with intensities that increase as the dopant level increases. These results strongly support the polaron formation through doping. On the other hand, at high doping levels, while the conductivity increases, the ESR intensity decreases with increasing dopant level, and new doping-induced absorption appears near the midgap ($\sim$1.55 eV). These results at high doping levels are in contrast to those of the photoexcitation experiments (see Table I). We have, therefore, proposed that for heavy doping, a confined positive soliton pair or bipolaron is formed via the process $P^+ + P^+ \rightarrow S^+ + S^+$ (or B^{2+}).

[1]S. Ichinose, Solid State Commun. **50**, 137 (1984).
[2]Y. Onodera, J. Phys. Soc. Jpn. **56**, 250 (1987).
[3]D. Baeriswyl and A. R. Bishop, J. Phys. C **21**, 339 (1988).
[4]D. Baeriswyl and A. R. Bishop, Phys. Scr. T **19**, 239 (1987).
[5]N. Kuroda, M. Sakai, Y. Nishina, M. Tanaka, and S. Kurita, Phys. Rev. Lett. **58**, 2122 (1987).
[6]N. Matsushita, N. Kojima, T. Ban, and I. Tsujikawa, J. Phys. Soc. Jpn. **56**, 3808 (1987).
[7]S. Kurita, M. Haruki, and K. Miyagawa, J. Phys. Soc. Jpn. **57**, 1789 (1988).
[8]S. Kurita and M. Haruki, Synth. Metals **29**, 129 (1989).
[9]K. Nasu and A. Mishima, Rev. Solid State Sci. **2**, 1 (1988).
[10]M. Tanaka, S. Kurita, T. Kojima, and Y. Yamada, Chem. Phys. **91**, 257 (1984).
[11]D. Baeriswyl, in *Theoretical Aspects of Band Structures and Electronic Properties of Pseudo-One-Dimensional Solids,* edited by H. Kamimura (Reidel, Dordrecht, 1985).
[12]A. J. Heeger, Philos. Trans. R. Soc. London, Ser. A **314**, 17 (1985).
[13]F. Baslo, J. C. Bailar, and B. R. Tark, J. Am. Chem. Soc. **72**,

2433 (1950).
[14]O. Bekaloglu, H. Breer, H. Keller, and H. N. Gung, Chim. Acta **21**, 183 (1977).
[15]Y. Yokoyama, M. Haruki, and S. Kurita (unpublished).
[16]Y. Hamaue, R. Aoki, M. Yamashita, and S. Kida, Bull. Chem. Soc. Jpn. **51**, 2234 (1978).
[17]Y. Wada, T. Mitani, M. Yamashita, and T. Kouda, J. Phys. Soc. Jpn. **54**, 3143 (1985).
[18]K. Nasu, J. Phys. Soc. Jpn. **53**, 427 (1984), and references therein.